Melatonin Maintains Macrophage M1 Phenotype to Reverse LPS-stimulated Tumor Immune Tolerance

Yukun Lin
Institute of Pharmacy, Pharmaceutical College of Henan University, Jinming District, Kaifeng, Henan Province 475004, China

Mengdi Zhang
Institute of Pharmacy, Pharmaceutical College of Henan University, Jinming District, Kaifeng, Henan Province 475004, China

Lin Zhou
Institute of Pharmacy, Pharmaceutical College of Henan University, Jinming District, Kaifeng, Henan Province 475004, China

Yuehua Wang
Institute of Pharmacy, Pharmaceutical College of Henan University, Jinming District, Kaifeng, Henan Province 475004, China

Mengqi Wang
Institute of Pharmacy, Pharmaceutical College of Henan University, Jinming District, Kaifeng, Henan Province 475004, China

Jincheng Du
Chinese Medical School, Hunan University of Chinese Medicine, Changsha, Hunan Province 410000,China.

Fuguang Kui
Institute of Pharmacy, Pharmaceutical College of Henan University, Jinming District, Kaifeng, Henan Province 475004, China

Wenwen Gu
Institute of Pharmacy, Pharmaceutical College of Henan University, Jinming District, Kaifeng, Henan Province 475004, China

Haihong Lin
Institute of Pharmacy, Pharmaceutical College of Henan University, Jinming District, Kaifeng, Henan Province 475004, China

Hong Li
Institute of Pharmacy, Pharmaceutical College of Henan University, Jinming District, Kaifeng, Henan Province 475004, China

Shihong Cen
School of Pharmacy and Chemical Engineering, Zhengzhou University of Industry Technology, Xinzheng, Henan Province 451150, China. 3 Chinese Medical School, Hunan University of Chinese

Medicine, Changsha, Hunan Province 410000,China
Gangjun Du (10200029@vip.henu.edu.cn)
Henan University

Research

Keywords: Melatonin, Macrophage polarization, LPS, Carcinogenesis, Immune surveillance

Posted Date: June 30th, 2020

DOI: https://doi.org/10.21203/rs.3.rs-37928/v1

Abstract

Background: Lipopolysaccharide (LPS) is a potent trigger of macrophage-mediated inflammation and its repeated stimulation results in immune tolerance. This study is to explore the cellular mechanisms of LPS-mediated tumor immune tolerance and to investigate whether melatonin can reverse this tolerance.

Methods: The effect of melatonin and LPS on macrophages was assessed by cell proliferation, morphological changes, phagocytosis and autophagy in vitro. The tumor-preventing effect of melatonin and LPS were evaluated in the urethane-induced lung carcinoma model and in the H22 liver cancer allograft model. Immunofluorescence, immunohistochemistry and ELISA were used to examine protein expression. The related targets and pathways of melatonin were predicted by comprehensive bioinformatics, and the clinical association of bacterial infections and survival was evaluated in cancer patients by meta-analysis.

Results: In vitro Raw264.7 macrophages were polarized toward the M1 phenotype by single LPS administration but toward the M2 phenotype by repeated LPS administration. Interestingly, combination treatment with repeated LPS and 10 μM melatonin prevented macrophage polarization toward the M2-like phenotype and exerted lasting antitumor efficacy. In the urethane-induced lung carcinoma model, repeated LPS administration stimulated macrophage polarization toward the M2 phenotype and promoted lung carcinogenesis, which was abrogated by macrophage depletion, while melatonin alone or in combination with repeated LPS challenge restored M1-like macrophages and prevented carcinogenesis. In the H22 liver cancer allograft model, melatonin maintained the macrophage phenotype and promoted the tumor-suppressing effect of repeated LPS challenge. Furthermore, we found that macrophages repeatedly stimulated with LPS had a high level of surface lipid rafts that mediated PI3K/AKT and JAK2/STAT3 signaling and prevented both LPS sensitivity and immune response by self-expression of PD-L1 and surface expression of PD-1 receptor on NK cells, whereas melatonin decreased surface lipid rafts and PI3K/AKT and JAK2/STAT3 signaling. Finally, we conducted a comprehensive bioinformatics analysis of melatonin-relevant targets and pathways involved in M2 macrophage polarization and evaluated the clinical associations of bacterial infections and survival in cancer patients.

Conclusions: This study suggests a function of melatonin in regulating macrophage polarization to maintain LPS-stimulated tumor immune surveillance.

Background

Cancer is one of the leading causes of human disease-related death, and much attention regarding cancer treatment has focused on targeting and killing the tumor itself, e.g. radiation, chemotherapy and targeted therapy.[1–5] Recently, cancer immunotherapy has become one of the most promising therapeutic pillars in improving patient survival.[6.7] Unlike other cancer treatments, cancer immunotherapy activates the host's immune system or relieves "immune exhaustion" in the tumor environment to eliminate cancer

cells.[8] The 10-year datasets from first-line anti-CTLA4 therapy show an unprecedented long-term survival in 20% of terminal metastatic melanoma patients that had never been seen before with other approaches to cancer treatment, indicating an exciting success in cancer immunotherapy that can provide hope of becoming “super-survivors” to incurable cancer patients[9.10]. Nevertheless, response rates with the most promising immunotherapy, such as PD-1 inhibitors, which represent immune-checkpoint-blockade(ICB)-mediated rejuvenation of exhausted T cells, only exhibit a modest 20% overall survival benefits in many solid tumors, whereas CAR-T cell therapy was reported to result in cerebral edema and cytokine release storms[7.11]. In addition, a more recent clinical report showed that PD-1 inhibitors could speed up tumor growth and promote tumor hyperprogression in 9% of cancer patients, indicating a need to optimize cancer immunotherapeutic approaches.[12] Current immunotherapies mainly activate tumor-infiltrating T lymphocytes and natural killer cells without regard to environmental changes that can cause various states of T cell dysfunction, such as anergy, tolerance, exhaustion, and senescence.[12.13] In fact, antitumor T cell immunotherapies originally exhibited responses but subsequently became resistant during prolonged antigen exposure due to “immune exhaustion” induced by the immunosuppressive microenvironment that is shaped by tumor-associated inflammatory cells. [14] Obviously, effective tumor immune rejection relies not only on antigen exposure-induced adaptive immune responses but also on the innate immune surveillance-regulated microenvironment.[15]

Tumor-infiltrated macrophages (TIMs) are a major inflammatory cell infiltrating the tumor microenvironment and are responsible for the immunosuppressive microenvironment and tumor progression.[16] Recent studies have shown that the inhibition of macrophage-mediated phagocytosis is an essential mechanism for tumor immune evasion.[17] In the clinic, TIMs are positively associated with high tumor grade and poor prognosis in various cancers. In mouse cancer models, TIM depletion or reeducation can reverse their tumor-promoting functions.[18.19] In addition, some recent reports have shown that innate macrophages also play important roles in the intratumor infiltration of CD8 cytotoxic T cells and the establishment of the long-lived memory lymphocytes. Therefore, targeting TIMs to reawaken innate immunity has emerged as a new cancer immunotherapy strategy.[20]. It is well known that activated macrophages are divided into antitumor M1 and protumor M2 phenotypes.[21] LPS can polarize macrophage toward the M1 phenotype, but repeated stimulation results in immune tolerance.[22] Melatonin is a neurohormone secreted by the pineal gland, This study explored the cellular mechanisms of LPS-mediated tumor immune tolerance and investigated whether melatonin can reverse this tolerance. [23]Our results are the first to indicated a vital role of macrophage polarization in LPS tolerance and also suggests a new mechanism by which bacterial infections increase the risk of carcinogenesis.

Materials And Methods

Materials.

Melatonin (purity > 98%) was purchased from Lianshuo biotechnology Co., Ltd. (Shanghai, China). Urethane, LPS and filipin were purchased from Sigma Chemical Co (St. Louis, MO, USA). Anti-F4/80-coated beads were purchased from BioCep (Israel). Antibodies used included anti-mouse-arginase, anti-mouse-iNOS, anti-mouse-F4/80, anti-mouse-CD8, anti-mouse-Foxp3, Cy3-conjugated anti-mouse CD86, PE-conjugated anti-mouse CD163 and FITC-conjugated goat anti-mouse IgG were obtained from BD Pharmingen or Proteintech (Shanghai China). Horseradish peroxidase (HRP)-conjugated goat anti-mouse IgG polyclonal antibody and peroxidase substrate DAB (3, 3'-diaminobenzidine) were obtained from Nichirei Bioscience (Tokyo, Japan).WP1066, DCFH-DA ,MβCD and LY294002 were obtained from Beyotime (Shanghai China). Mouse quantitative ELISA kits (IFN-γ, IL-12, IL-10, TGF-β1, arginase 1 and ROS) were obtained from R&D Systems. L-arginine and nitric oxide assay kits were obtained from Nanjing Jiancheng Bioengineering institute. Standard rodent chow was purchased from Henan Provincial Medical Laboratory Animal Center (Zhengzhou, China), License No. SCXK (YU) 2015-0005, Certificate No. 41000100002406. Liposome-encapsulated clodronate (LEC) was prepared as described previously. [24]

Cell Culture and Assay

Raw264.7 macrophages and the Lewis lung carcinoma (LLC) cells were from ATCC, purchased from the Chinese Academy of Sciences and grown in RPMI1640 medium supplemented with 10% (v/v) fetal bovine serum (FBS) in a humidified atmosphere containing 5% CO_2 and 95% air at 37℃. Raw264.7 macrophages were seeded in 24-well plates and stimulated with by 10 ng/ml LPS or 10 ng/ml IL-10 for 24 h to obtain M1-like (M1) and M2-like (M2) macrophages. To collect cell-conditioned media, M1-like or M2-like cells were cultured in serum-free medium for 24 h, centrifugated to remove the cells and further filtered to remove debris for supernatant collection as M1 and M2 cell-conditioned media(M1-CM and M2-CM,respectively). The supernatant levels of IFN-γ, TNF-α, NO, PD-L1, IL-10 and TGF-β1 were determined by ELISA kits, according to the manufacturer's protocols.[25] The results were calculated from linear curves obtained by using the Quantikine kit standards.

For proliferation analysis, LLC cells at 1×10^5 cells/mL were seeded in a 96-well plate and treated with M1 or M2 cell-conditioned media for 48 h, M1-like or M2-like cells were also treated with LPS or melatonin alone or in combination for 7 d (changing the medium every 2 days), and living cells were examined by MTT reduction assay, according to our previous method.[24] For the morphological assessment, the cells were analyzed by a Laser holographic cell imaging and analysis system (HoloMonitor M4, Phiab, Sweden).[25] For phagocytic ability assessment, neutral red phagocytosis was detected. For autophagy analysis, the cells were stained using PE-conjugated anti-LC3-B or anti-p62 antibodies. For apoptosis analysis, the binding of ANXV-FITC to phosphatidylserine was measured by an automated cell counter and analysis system (Nexcelom Cellometer X2, Nexcelom, USA). For ROS measurement, intracellular fluorescence of DCFH-DA was detected by a fluorescence spectrophotometer(F4600, Hitachi,Japan). For lipid raft detection, cells were then stained with filipin (0.05 mg/ml) for plasma membrane cholesterol, respectively according to conventional methods.

Western blot analysis

M1-like and M2-like macrophages were treated with LPS or melatonin alone or in combination in the presence or absence of MβCD (a lipid raft inhibitor),WP1066 (a selective JAK2/STAT3 inhibitor) or LY294002 (a PI3k/AKT inhibitor) for 48 h. The protein was extracted in cell lysis buffer, and equal amounts of protein were separated via 12% sodium dodecyl sulfate-polyacrylamide gel electrophoresis, electroblotted onto nitrocellulose membranes, and probed with antibodies against PD-1, PD-L1, JAK2, pAKT, and Stat3. Antibody binding was detected via enhanced chemiluminescence according to the manufacturer's instructions (Pierce, Rockford, IL). Band density was quantified using ImageJ software (NIH, Bethesda, MD, USA) and normalized to the corresponding control group.

Animals

Ten-week-old female ICR mice were obtained from Henan Provincial Medical Laboratory Animal Center. All mice were housed in individual ventilated cages (lights on 7:00 AM to 7:00 PM). Animals were fed standard rodent chow and water. All animal procedures were approved by the Animal Experimentation Ethics Committee of Henan University (permission number: HUSAM 2016 – 288), and all procedures were performed in strict accordance with the Guide for the Care and Use of Laboratory Animals and the Regulation of the Animal Protection Committee to minimize suffering and injury. Animals were euthanized via carbon dioxide overdose based on experimental needs.

LLC cell immune clearance

LLC cell immune clearance was assessed using a calcein-release assay, according to our previous method.[24] Briefly, NK cells (DX5+) were purified from the ICR mouse spleens using the MACS separation system (Miltenyi Biotec, Bergisch Gladbach, Germany), stimulated with IL-2 (10 ng/ml) for 24 h in the presence of M1-like or M2-like cell-conditioned media and harvested as attacking cells. Mitomycin C-treated LLC cells were labeled with 10 μM calcein-AM as target cells and were placed into a 96-well plate with CD8 + T cells at 100:1, 50:1, and 25:1 (NK cells:LLC cells) ratios for 6 h at 37 °C. The supernatants were transferred from each well to another 96-well plate, and the fluorescence was measured using a Synergy2 multimode microplate reader (BIO-TEK). Maximum release was obtained from detergent-released LLC cells, and spontaneous release was obtained from LLC cells incubated in the absence of CD8 + T cells (n = 5).

Immune clearance was determined as follows:

Immune clearance = (experimental release – spontaneous release) / (maximum release – spontaneous release) × 100%.

To detect how the different macrophage phenotypes affect NK cells, NK cells were cultured in the lower chamber at a concentration of 5×10^6 cells/ml and were stimulated with IL-2, and M1-like or M2-like cells were added in the upper chamber at 2×10^6 cells/ml in the presence or absence of anti-IL-10, anti-TGF-β1, MβCD, WP1066 or LY294002. After coincubation for 24 h at 37 °C, the supernatant was centrifugated for the PD-L1 assay, adherent cells in the upper compartment were removed by a cotton swab, and the filter inserts were incubated in medium supplemented with 5 mg/ml DAPI for 30 min at 37 °C and analyzed for

cell migration using an inverted fluorescence microscope. NK cells in the lower chamber were collected for surface PD-1 receptor assay using PE-conjugated anti-PD-1 antibody.

Cytolytic assay

The cytolytic activity of LLC cells was assessed by CFSE-7AAD staining. Briefly, LLC cells were incubated with CFSE -labeled M0, M1-like or M2-like cells at 20:1 and 10:1 (M0, M1 or M2 cells: LLC cells) ratios for 6 h. Then, 7AAD was added to the cell suspensions and incubated on ice for 15 min. The percentages of 7AAD + cells among CFSE + cells were analyzed using an automated cell counter and analysis system.

Urethane-induced lung carcinogenesis model

Urethane (600 mg/kg body weight), alone or in combination with liposome-encapsulated clodronate (LEC, 4 mg/mouse) was injected intraperitoneally (i.p.) into ICR mice once a week for eight weeks, according to our previous protocol.[26] Following the first urethane injection, mice received melatonin (20 mg/kg/day) via intragastric administration once a day or LPS (1 mg/kg/day) via intravenous tail injection once a week alone or in combination for twelve weeks. At thirteen weeks after the first urethane injection, orbital venous blood was collected for serum assays of IFN-γ, IL-2, TNF-α,PD-L1, IL-10 and TGF-β1 using an ELISA kit. The mice were sacrificed, and cell-free alveolar fluid was collected by inserting a cannula into the trachea with three sequential injections of 1 mL PBS, followed by centrifugation, for cytokine assay (IFN-γ, IL-2, TNF-α, ROS, IL-10 and TGF-β1), while the separated cells were resuspended in 0.9% sterile saline for total cell counts. Macrophages in the suspensions were enriched by magnetic cell sorting utilizing anti-F4/80-coated beads, and macrophage immunophenotypes were analyzed by FITC-conjugated anti-mouse CD86 and CD163 staining using an automated cell counter and analysis system (Nexcelom Cellometer X2, Nexcelom, USA).

Spleen NK cells (DX5+) were separated using the autoMACS separation system for assays of surface PD-1 receptor and memory NK cell rate (NKG2c + NKG2a-) using an automated cell counter and analysis system.

The average numbers of lung carcinomas per mouse were calculated. A portion of each lung was preserved in 10% buffered formalin and routinely embedded in paraffin. Lung sections were stained by immunohistochemistry and immunofluorescence according to our previous method.[27] After overnight incubation with the primary antibodies (anti-PD1, anti-iNOS, and anti-CD31), the slides were incubated with the FITC-conjugated goat anti-mouse IgG for 30 minutes. The total immunohistochemical and immunofluorescence scores were calculated by the intensity score and proportion score by excluding the primary antibody and IgG matched serum, respectively, as positive and negative controls.

In addition, the lung vascular integrity was assayed by the Evans blue dye extrabarrier technique according to our previous method.[28]

Tumor allograft model

H22 cells were used for tumor allograft experiments. Two hundred microliters of saline containing 1×10^6 cells were injected subcutaneously into the lateral axilla of mice to establish tumor allografts. One day after tumor inoculation, in vitro LPS-induced M1 or IL-10-induced M2 cells (2×10^6 cells in 200 μL saline) were injected intravenously into mice once a week for three weeks; simultaneously, mice received melatonin (20 mg/kg) via intragastric administration once a day and LPS (1 mg/kg) or LEC (4 mg/mouse) via intravenous tail injection once a week alone or in combination for 3 weeks. Tumor size was monitored twice a week with calipers and calculated as the length x width^2 /2. On the twenty-second day after tumor inoculation, orbital venous blood was collected for serum assays of IFN-γ, IL-2, TNF-α,PD-L1, IL-10 and TGF-β1. The mice were euthanized, the tumors were extracted and weighed, peritoneal macrophages were enriched by magnetic cell sorting utilizing anti-F4/80-coated beads, and macrophage immunophenotypes were analyzed. Spleen NK cells were separated using the autoMACS separation system for assays of surface PD-1 receptor and memory NK cell rate. The complete assay procedure was similar to the methods in the urethane-induced lung carcinogenesis model.

In addition, the tumor vascular integrity was assayed with the Evans blue dye extrabarrier technique according to our previous method.[25]

For the immune rechallenge study, the tails of 1/2 of the 40 mice were injected subcutaneously with 5×10^5 H22 cells suspended in 50 μl saline. One day after tumor inoculation, the mice received melatonin (20 mg/kg) via intragastric administration once a day and LPS (1 mg/kg) or LEC (4 mg/mouse) via tail intravenous injection once a week alone or in combination for 2 weeks. Fifteen days after tumor implantation, the tumor-bearing tail was cut off to remove the primary tumor, and the mice were rechallenged with subcutaneous injections of 1×10^6 H22 cells in 200 μl saline in the flanks, while 10 normal mice were challenged with identical H22 cells. Tumor size was monitored twice a week with calipers. At thirty-six days, the same detections as above were carried out.

The regulatory mechanism of melatonin on neutrophils

The gene expression profiles GSE5099 were obtained from the Gene Expression Omnibus (GEO) database, Up- and downregulated genes related to tumor-associated macrophages were identified using GEO2R, and the human structures of these differential proteins were collected from the protein data bank (PDB) for docking analysis. The chemical structure of melatonin was obtained from PubChem, and the docking exercise was conducted using the online software systemsDock with the autoremoval of unspecified protein structures. Docking scores over 5 were regarded as the potential targets for melatonin. Gene ontology (GO) and Kyoto Encyclopedia of Genes and Genomes (KEGG) enrichment analyses were performed for the potential targets using the Database for Annotation, Visualization and Integrated Discovery (DAVID) and the online software Omicshare. The protein-protein interactions (PPIs) among these potential targets were constructed using the STRING database, and the hub genes were identified using Cytoscape.

Network Meta-analysis

We systematically searched PubMed and Web of Science to identify eligible studies published from Jan 1, 1990 to Apr 1, 2019. OR and hazard ratios (hrs) with 95% confidence intervals (cis) were used to evaluate the risk of bacterial infections in carcinogenesis and cancer survival. Fixed and random-effect meta-analyses were conducted based on the heterogeneity of the included studies. To minimize case selection bias, sensitivity analyses were performed.

Statistical analyses

The data were statistically analyzed using GraphPad Prism, Version 5.0 (San Diego, CA, USA) and are presented as the mean ± SD. The differences between two groups were evaluated using a t-test. A P value of less than 0.05 was considered statistically significant. Meta-analyses were performed using the fixed-effects inverse-variance method using RevMan 5.3. Heterogeneity was calculated using the I^2 statistics and chi-square Q test, and a *P*-value of heterogeneity < 0.10 or I^2 >50% indicated significant heterogeneity. Usually, a fixed-effect model was used, and the random-effects model was adopted when the heterogeneity was significant.

Results

M2 macrophages had an opposing effect on LLC cells compared to that of M1 macrophages

It was reported that cancer-associated macrophages have M2-like characteristics and exert tumor-promoting actions, unlike M1-like macrophages, which show antitumor functions.[29] To explore these properties, we induced the polarization of Raw264.7 macrophages into M1-like cells and M2-like cells. As expectedly, compared to the characteristics of M1-like cells, M2-like cells had high levels of surface CD163 expression (Fig. 1A, 1B) with morphological changes indicated by the cell distribution (Fig. 1D, 1E). In neutral red phagocytosis, there was no difference between M1 and M2 cells (Fig. 1C); however, M2-like cells had a reduction in ROS indicated by intracellular fluorescence of DCFH-DA (Fig. 1F) and an increase in autophagy indicated by LC3-B and p62 immunofluorescence (Fig. 1H). When cocultured with M1 cell-conditioned media (M1-CM), LLC cells showed reduced proliferation (Fig. 2B) and increased apoptotic rates (Fig. 2C), which were not affected by M2 cell-conditioned media (M2-CM). Consistent with these results, M1-like cells led to LLC cell lysis (Fig. 2D), which was not influenced by M2-like cells, and M1 cell-conditioned media promoted LLC cell immune clearance (Fig. 2D) which was prevented by M2-CM.

M2 macrophages had the more lipid rafts and suppressed NK cells

It is well known that high TIMs and low NK cells may be associated with an poor prognostic survival in cancer patents[30]. To explore how macrophages affect NK cells, we detected differences between M1-like and M2-like macrophages and their influence on NK cells. M2 cells had the more lipid rafts, as indicated

by membrane cholesterol (Fig. 2I) ang produced more PD-L1 (Fig. 2G) and JAK2/STAT3 activation (Fig. 2G) compared to those of M1 cells. M1-CM promoted immune clearance of LLC cells by NK cells (Fig. 2E), which was prevented by M2-CM. Consistent with these results, M2 cells promoted NK cell expression of PD-1 surface receptor (Fig. 2F), and MβCD and anti-TGF-β1 antibody but not anti-IL-10 antibody prevented M2 cells from inducing PD-L1 production and NK cells from expressing PD-1, whereas JAK2/STAT3 signal blockade by WP1066 but not PI3K/AKT signal blockade decreased M2 cell lipid rafts and PD-L1 production(Fig. 2G,2H).

Melatonin reverses the macrophage tolerance of LPS

Macrophages may be tolerant to LPS, an effect that lasts for a period of time.[31] To explore how macrophages become tolerance to LPS, we observed the effects of melatonin and LPS on macrophage polarization. As expected, repeated LPS treatment led to macrophage tolerance of LPS (Fig. 1A) accompanied by a shift from the M1 to M2 phenotype, the increased lipid rafts and the JAK2/STAT3 activation (Fig. 2G, 2H), while no more than three stimulations induced macrophage polarization toward the M1 phenotype (Fig. 1A). Unexpectedly, when administered at the dose (10 μM), which had a small effect on cell viability in M1 cells (Fig. 2A), melatonin improved the morphological changes indicated by cell distribution (Fig. 1D, 1E) and induced apoptosis in M2 cells (Fig. 2A) with the increased ROS (Fig. 1F) and the decreased autophagy (Fig. 1H), accompanied by suppression of lipid rafts and JAK2/STAT3 signaling. Importantly, the combination treatment with LPS and melatonin resulted in the polarization of macrophages toward M1 cells (Fig. 1A). Furthermore, we found that both of lipid raft depletion by MβCD and JAK2/STAT3 signal blockade by WP1066 attenuated the effect of melatonin on M2 cells (Fig. 2F, 2H).

Melatonin maintains macrophage M1 phenotype to reverse LPS-mediated carcinogenesis in a urethane-induced lung cancer model

To confirm the roles of macrophages in carcinogenesis, we investigated macrophage phenotypes in a urethane-induced mouse lung cancer model, which is usually used for studying basic lung tumor biology and finding new tumor intervention strategies. In this study, the mice received melatonin or LPS for twelve weeks. At thirteen weeks, lung cancer nodes were visible to the naked eye (Fig. 3A). The number of lung cancer nodes was 26.2 ± 4.1, regardless of the heterogeneity of tumor histology in the control group (Fig. 3B). As expected, macrophage infiltration in alveolar cavities was positively correlated with lung carcinogenesis in the control group (Fig. 3C, 3D, 3E, 3F), and both of melatonin treatment and macrophage depletion induced by LEC prevented lung carcinogenesis (Fig. 3A, 3B). Unexpectedly, LPS alone did not prevent lung carcinogenesis but promoted these incidents (Fig. 3A, 3B). Immunophenotypes showed that the infiltrated macrophages were similar to IL-10-treated Raw264.7 macrophages and expressed more surface CD163 in the control group (Fig. 3E, 3F), indicating an M2 phenotype. ELISA showed that the levels of IFN-γ, IL-2, and TNF-α decreased, while the levels of IL-10 and TGF-β1 increased in serum and in alveolar cavities in control mice compared to those of normal mice (Fig. 3G, 3H),

indicating immune tolerance. These changes were promoted by repeated LPS administration and were attenuated by melatonin. Importantly, the combination of LPS and melatonin maintained the M1 phenotype (Fig. 3D, 3F) and reverses the lung carcinogenesis-promoting effect of LPS (Fig. 3A, 3B), accompanied by a reduction in serum PD-L1 levels (Fig. 3G), spleen NK cell surface PD-1 expression(Fig. 4C), lung tissue immunohistochemical staining of PD-1, iNOS, immunofluorescence staining of CD31 (Fig. 4A, 4B), and permeability to evans blue dye (Fig. 4E), as well as an increase in spleen memory NK cells (Fig. 4D) and NK cell surface PD-1 expression rates (Fig. 4C), indicating a better immune restoration and lung vascular integrity.

Melatonin maintains the macrophage M1 phenotype to promote LPS-induced tumor suppression and to reverse repeated LPS-induced immunosuppression in the H22 liver cancer allograft model

To further confirm the roles of macrophages in tumor progression, we established an allograft model of H22 liver cancer and injected M1 and M2 cells via the tail vein into tumor-bearing mice. The M2 cell injection promoted tumor growth, whereas the M1 cell injection prevented tumor growth (Fig. 5A, 5B), indicating protumor and antitumor functions of macrophages, respectively. Unlike the results of the urethane-induced lung cancer model, in this allograft model, melatonin (20 mg/kg) or macrophage depletion had a negligible suppression on tumor growth, while LPS showed a significantly suppressive effect on tumor growth (Fig. 5A, 5B). The tumor-suppressing efficacy of LPS was promoted by melatonin, macrophage depletion and M1 cell injection, which decreased the intratumor permeability of evans blue dye (Fig. 5C) but was attenuated by M2 cell injection (Fig. 5A, 5B), which increased the intratumor permeability of evans blue dye. Immunophenotyping showed that the infiltrated macrophages were similar to IL-10-treated Raw264.7 macrophages and expressed more surface CD163 in the control group, indicating an M2 phenotype (Fig. 5D). The results of serum cytokines (Fig. 5G) and spleen NK cell analyses (Fig. 5E, 5F) were similar to those in the urethane-induced lung cancer model, indicating an M2 macrophage-polarizing effect of repeated LPS. The immunosuppressive efficacy of repeated LPS-induced macrophages was further confirmed in an H22 cell rechallenge immune study where tumor immune rejection was suppressed by repeated LPS stimulation, while it was promoted by melatonin. Importantly, the combination of LPS and melatonin synergistically stmulated immune rejection of H22 cells (Fig. 6A), accompanied by a reduction in peritoneal M2 macrophages (Fig. 6B), serum levels of PD-L1, IL-10 and TGF-β1(Fig. 6E), and spleen NK cell surface PD-1 expression (Fig. 6C) and an increase in peritoneal M1 macrophages (Fig. 6B), serum levels of IFN-γ, IL-2, TNF-α (Fig. 6E), and spleen memory NK cell rate (Fig. 6D), indicating a sustained effect of melatnin on the M1 macrophage phenotype. The immune-rejecting efficacy of melatonin on tumor rechallenge could be aborgated by macrophage depletion, indicating an important role of macrophages in secondary immunity and immune memory.

Melatonin regulates macrophages by targeting the multi-protein network

We queried 590 upregulated genes (LogFC ≥ 1.5, $P < 0.05$) and 994 downregulated genes (LogFC ≤-1.5, $P < 0.05$) related to M1-associated macrophages and obtained 181 targets. A total of 136 potential targets

with a docking score > 6.0 (pKd/pKi) were selected for GO and KEGG analyses (Fig. 8, Fig. 7A). A hypergeometric distribution count > 4 and $P < 0.05$ were set as threshold criteria to identify the functional gene ontology and pathways. GO enrichment analysis indicated that the potential targets of melatonin were primarily associated with the “signal transduction”, “innate immune response”, “cell proliferation”, “protein phosphorylation” and “apoptotic process” terms (Fig. 8). KEGG enrichment analysis revealed that the potential targets of melatonin were significantly enriched in the “Pathways in cancer”, “TNF signaling pathway” and “JAK/STAT signaling pathway” terms (Fig. 7C). The PPI network identified 4 key genes (JAK2, STAT3, PIK3CA, and AKT1) that were hub genes for melatonin (Fig. 7B). These results were confirmed by Western blot analysis **(**Fig. 2F, 2G, 2H**)**.

Bacterial infection increases the risk of carcinogenesis and is adversely associated with survival times in cancer patents.

A total of 5 epidemiologic surveys and 24 observational clinical articles (8 prospective studies and 21 retrospective studies) including 4406 patients were included in the meta-analysis. Bacterial infection significantly increased the risk of carcinogenesis (OR = 2.76, 95% CI: 2.58–294; P = 0.00001) **(**Fig. 9A**).** According to the 14 articles concerning antibiotic therapy which included 3346 participants, we found that the antibiotic therapy significantly improved survival in cancer patients (HR = 0.76, 95% CI: 0.71–0.8; P = 0.00001), especially in leukemia patients (HR = 0.73, 95% CI: 0.66–0.81; P = 0.0002) **(**Fig. 9C **and D)**, indicating a prediction role of bacterial infection in risk of cancer survival. In the subgroup analysis, gastric cancer patients got the risk with helicobacter pylori infection(15 studies with 3108 patients) (OR = 1.94, 95% CI: 1.74–2.17; P = 0.00001) **(**Fig. 9A **and B)**, colon cancer patients got the risk with salmonella infection(5 studies with 320 patients) (OR = 6.87, 95% CI: 6.11–7.13; P = 0.16) **(**Fig. 9A **and B)**, which may be associated with bacterial infection-induced the shift of anti-tumor M1 type macrophages into pro-tumor M2 type macrophages.

Discussion

Cancer may arise from alterations in different physiological processes and is refractory to cure due to unknown etiology and genetic heterogeneity. Based on self-healing ability, immunotherapy has been great expectation against distinct types of cancer.[32–37] Current immunotherapies targeting different cellular checkpoint controllers emerged as having either innate or acquired resistance due to the immunosuppressive tumor environment, guiding the direction of developing cancer immunotherapy.[38] The object of cancer immunotherapy is to stimulate a long-lasting immunosurveillance, maintaining the antitumor immunity.[39] Macrophages, as the first-line immune responders in the innate immune system, are responsible for nonresolving inflammation in tumors. Understanding the roles of macrophages in the tumor immune response may help develop new immunotherapeutic strategies and enhance the response rate of immunotherapy.[40] Macrophages can exhibit both pro- and antitumorigenic properties, depending on their phenotype. Recent studies have demonstrated that targeting TIMs can reverse the immunosuppressive tumor microenvironment and stimulate robust tumor-specific immune responses, which is consistent with the fact that immunosuppressive TIMs are abundant in the tumor

microenvironment and are positively correlated with poor prognosis. Therefore, maintaining the antitumorigenic phenotype of macrophages rather than completely depleting TIMs represents a new cancer immunotherapy strategy.[41.42] LPS is a potent trigger of macrophage-mediated inflammation and has been recognized as a potent antitumor agent in animal tumor models.[42] However, its use in human cancer therapy was not very successful due to LPS-induced tolerance, a state of altered responsiveness in macrophages, which results in poor tumor response and is a major cause of secondary hospital infections. Previously, Boris et al reported that β-glucan could reversed the epigenetic state of LPS-induced immunological tolerance to reduce overall sepsis mortality.[22.43] In this study, we first showed that the combination of LPS and melatonin could prevented macrophage polarization toward M2-like cells and therefore exerted a lasting antitumor efficacy, suggesting a novel effective strategy for reversing LPS tolerance.

Macrophages can be activated in response to different agents to become M1 and M2 macrophages and thus exert different functions. It is well known that LPS is able to polarize macrophages toward the M1 phenotype, which exerts the proinflammation and antitumor effects.[44] Consistent with these functions, in an animal model, LPS demonstrated a therapeutic effect on the transplanted tumor with inhibition of tumor size and growth. In small clinical trials, LPS also led to cancer remission and disease stabilization in cancer patients.[45.46] However, LPS is responsible for the biological properties of bacterial endotoxins, which are potent inflammagens and result in fever, septic shock, toxic pneumonitis, and respiratory symptoms; however, a cohort study found that long-term exposure to endotoxin was associated with a reduced risk of lung cancer.[46.47] In goats, LPS treatment triggered an excessive inflammatory response and elevated the body temperature to 40 °C.[48] In clinical trials, even pretreated with ibuprofen resulted in the unavoidable LPS-mediated clinical toxicities.[49] In addition, subsequent LPS-induced macrophage resistance after activation was also an obstacle that prevented durable tumor response to macrophages. Despite intense investigations of various epigenetic and genetic changes in tolerant macrophages for many years, a unifying mechanism that is responsible for LPS tolerance remains elusive.[50–52] Jo¨rg et al used genome-wide transcriptional profiling technology to show the hyporesponsiveness of most LPS target genes in tolerant macrophages.[53] In the present study, Raw264.7 macrophages were polarized toward M1-like cells by a single LPS challenge but toward M2-like cells by repeated LPS challenge, suggesting a critical process of LPS tolerance in macrophages. The meta-analysis showed that bacterial infection increases the risk of carcinogenesis and is adversely associated with cancer survival, suggesting a wide role of LPS tolerance in cancer progression. A mechanistic understanding of the role of LPS in tumor progression will provide unique therapeutic alternatives.

Melatonin is a pleiotropic molecule and has numerous physiological and pharmacological actions.[54.55] Melatonin generally plays a check-and-balance role in immunity and inflammation. Melatonin is an immunostimulator that drives an activated immunocyte state in favor of effectively clearing pathogens under normal or immunosuppressive conditions, while it acts as an immunosuppressor that urges immunocytes to enter an inactivated state that suppresses inflammatory reactions under excessively inflammatory conditions.[56.57] Several studies found that melatonin had an exciting potential to override

the immunosuppressive tumor environment. [58]Various reports have shown that melatonin promotes 80% survival in lethal LPS-treated mice and significantly reduces the LPS-treated mortality in mice and rats by correcting the LPS-induced inflammatory imbalance with decreased levels of NO and lipid peroxidation.[59.60] In addition, a recent study demonstrated that melatonin cold suppresses indoleamine 2,3-dioxygenase-1 (IDO1) (a key immunomodulatory enzyme associated with cancer immune escape) to overcome tumor-mediated immunosuppression. [61.62] Based on these results, we believe that the combination of LPS and melatonin can maintain macrophage sensitivity to LPS and simultaneously limit excessive pathogenic stimuli to avoid a “macrophage exhaustion” phenotype. Consistent with our hypothesis, in this study, the combination of LPS and melatonin resulted in optimal cancer prevention in a urethane-induced lung carcinogenic model and H22 liver cancer allograft model without significant side effects. Furthermore, we found that macrophages repeatedly challenged with LPS had a high level of surface lipid rafts and JAK2/STAT3 activation, which prevented both M1-like polarization and immune responses, whereas melatonin decreased surface lipid rafts and JAK2/STAT3 signaling. Bioinformatics analysis found that the potential targets of melatonin regulation of macrophages were primarily associated with the “inflammatory response”, “signal transduction”, “cell proliferation” “innate immune response” and “negative regulation of apoptotic process”, indicating a function of melatonin targeting multi-protein networks, such as “Jak-STAT signaling pathway”, “Toll-like receptor signaling pathway” and “Chemokine signaling pathway”, whereby melatonin maintains M1 macrophage phenotypes to reverse LPS-stimulated immune tolerance. We used a pharmacological blocker to confirm the important role of Jak-STAT signaling in the melatonin-maintained macrophage phenotype, and JAK2/STAT3 signal blockade prevented M2-like macrophages from producing PD-L1 and NK cells from expressing PD-1, whereas lipid raft depletion decreased M2-like macrophage JAK2/STAT3 signaling, indicating an association of M2 macrophage functions and the feedback loop of lipid rafts - JAK2/STAT3-PD-L1. Certainly, this is only one of the important feedback loops.

Historically, bacterial therapy as oncolytic agents has been recognized for malignant brain tumours, which showed an extended survival times for patients who developed infections at the site of resection of malignant gliomas, and cancer vaccines were assumed to be based on immunotoxins of bacterial origin. [63] It was previously reported that occupational exposure to endotoxin in organic material reduced the risk of lung cancer among workers employed $\leq$ 35 years but increased the risk of lung cancer among those employed > 50 years, implying a cancer-promoting action of endotoxin tolerance. [64.65] In fact, LPS (also referred to as endotoxin) as a cell wall component of gram-negative bacteria has been used for tumor destruction for many years, such as a report by Chicoine et al that intratumor injection of LPS could cause the regression of subcutaneously implanted mouse glioblastoma multiforme in animal tumor models. [66] Goto S et al also reported that three of five evaluable human cancers showed a significant response to intradermal LPS administration, suggesting that LPS is a potent antitumor agent. [67] However, only one trial of LPS use in human cancer therapy declared a poor tumor response and unbearable side effects. In addition, LPS inhalation can also produce both a systemic and a bronchial inflammatory response. [68.69] Therefore, it is necessary for LPS use as an antitumor agent to balance its

inflammatory response and tolerance. Our study provides a safe and effective strategy for the clinical application of LPS, and this therapeutic strategy is worth investigating.

Conclusions

In summary, melatonin regulation of immune balance plays an important role in the LPS-stimulated macrophage response, and our findings suggest several potential clinical implications. First, M2 macrophage polarization correlates with LPS-stimulated “macrophage exhaustion”, supporting therapeutic targeting of TIMs in an immunosuppressive environment. Second, alteration of the macrophage phenotype is superior to depletion of TIMs for reversing LPS tolerance and tumor immunosuppression, indicating the potential of reeducating these cells to reverse their protumor functions for antitumor properties. Third, macrophages, as the first–line responders of innate immune surveillance, are needed not only for the initiation of tumor innate immune responses but also for the long-lasting preventive functions of NK cells against tumors, indicating the first priority for the development of efficient immunotherapies. Certainly, whether reeducating TIMs by the combination of melatonin and LPS is the most effective approach for restoring antitumor immune responses needs to be fully evaluated, and the dose-effect and exposure-timing relations also need also to be further investigated.

Declarations

Author Contributions

Conceived and designed the experiments: Gangjun Du.

Performed the experiments: Yukun Lin, Mengdi Zhang, Lin Zhou, Yuehua Wang, Mengqi Wang, Fuguang Kui, Wenwen Gu, Haihong Lin, Shihong Cen.

Analyzed the data: Gangjun Du, Yukun Lin, Haihong Lin, Shihong Cen, Hong Li.

Contributed reagents/materials/analysis tools: Gangjun Du, Haihong Lin, Hong Li.

Wrote the paper and plotted the results: Gangjun Du, Yukun Lin, Mengdi Zhang.

ACKNOWLEDGMENTS

Not applicable.

Conflict of interest

The authors have declared no conflict of interest.

Availability of data and materials

All data generated or analyzed during this study are included in this article.

Consent for publication

Not applicable

Ethics approval and consent to participate

This study was approved by Animal Experimentation Ethics Committee of Henan University (permission number HUSAM 2016-288), and all procedures were performed in strict accordance with the Guide for the Care and Use of Laboratory Animals and the Regulation of Animal Protection Committee.

Funding

This study was supported *by* Natural Science Foundation of Henan Province of China (No. 182300410310), Postgraduate Education Reform Project of Henan Province (No. hnyjs2015kc24), Postgraduate Education Innovation and Quality Improvement Project of Henan University (No. SYL18060137 and SYL18060136). We thank American Journal Experts (AJE) for language editing.

Publisher's Note

Springer Nature remains neutral with regard to jurisdictional claims in published maps and institutional affiliations.

Contributor Information

Yukun Lin, Email:15736880141@163.com

Mengdi Zhang, Email: zhangmengdi166565@163.com

Lin Zhou, Email: 13137591738@163.com

Yuehua Wang, Email: 13137596876@163.com

Mengqi Wang, Email: 13783602198@163.com

Jincheng Du,Email:jinchengd258@126.com

Fuguang Kui,Email:kfg157699@163.com

Wenwen Gu,Email:18360345223@163.com

Haihong Lin, Phone: 86-0371-23880680, Email: linhaihong369@126.com

Hong Li, Phone: 86-0371-23880680; E-mail：10200121@vip.henu.edu.cn

Shihong Cen,E-mail：e13936613673@163.com

Gangjun Du, Phone: 86-0371-23880680, Email: 10200029@vip.henu.cn

References

1. Jingting Liu, Chunyan Meng, Changcan Li. Deleted in breast cancer 1 as a novel prognostic biomarker for digestive system cancers: a meta-analysis. J Cancer. 2019;10(7): 1633–1641.
2. Xiaoliang Liu, Qingyu Meng, Weiping Wang. Predictors of distant metastasis in patients with cervical cancer treated with definitive radiotherapy. J Cancer. 2019;10(17): 3967–3974.
3. Phatsapong Yingchoncharoen, Danuta S. Kalinowski, Des R. Richardson. Lipid-based drug delivery systems in cancer therapy: What is available and what is yet to come. Pharmacol Rev. 2016;68(3): 701–787.
4. Li H, Wang S, Yue Z. Traditional Chinese herbal injection: Current status and future perspectives. Fitoterapia. 2018;129:249-256.
5. Rong J, Li L, Jing L. JAK2/STAT3 Pathway Mediates Protection of Metallothionein Against Doxorubicin-Induced Cytotoxicity in Mouse Cardiomyocytes. Int J Toxicol. 2016;35(3):317-326.
6. Alexander H. Morrison, Katelyn T. Byrne, Robert H. Vonderheide.Immunotherapy and prevention of pancreatic cancer. Trends Cancer.2018;4(6): 418–428.
7. Roberta Zappasodi,Taha Merghoub, Jedd D. Wolchok.Emerging concepts for immune checkpoint blockade-based combination therapies. Cancer Cell. 2018;33(4): 581–598.
8. E. John Wherry, Makoto Kurachi. Molecular and cellular insights into T cell exhaustion. Nat Rev Immunol. 2015;15(8): 486–499.
9. Paolo A Ascierto, Ester Simeone, Vanna Chiarion Sileni. Clinical experience with ipilimumab 3 mg/kg: real-world efficacy and safety data from an expanded access programme cohort. J Transl Med.2014;12: 116.
10. Zhang H, Jiang H, Zhang H. Anti-tumor efficacy of phellamurin in osteosarcoma cells: Involvement of the PI3K/AKT/mTOR pathway. Eur J Pharmacol. 2019;858:172477.
11. Daniel W. Lee, Rebecca Gardner, David L. Porter.Current concepts in the diagnosis and management of cytokine release syndrome. Blood.2014;124(2): 188–195.
12. Siwen Hu-Lieskovan, Antoni Ribas. New combination strategies using PD-1/ L1 checkpoint inhibitors as a backbone. Cancer J.2017;23(1): 10-22.

13. Sun Z, Ren Z, Yang K. A next-generation tumor-targeting IL-2 preferentially promotes tumor-infiltrating CD8+ T-cell response and effective tumor control. Nat Commun. 2019;10: 3874.
14. Li J, Lee Y, Li Y. Co-inhibitory molecule B7 superfamily member 1 expressed by tumor-infiltrating myeloid cells induces dysfunction of anti-tumor CD8+ T cells. Immunity.2018;48(4):773-786.
15. Leticia Corrales, Vyara Matson, Blake Flood. Innate immune signaling and regulation in cancer immunotherapy. Cell Res. 2017;27(1): 96–108.
16. Huayang Wang, Qianqian Shao, Jintang Sun. Interactions between colon cancer cells and tumor-infiltrated macrophages depending on cancer cell-derived colony stimulating factor 1. Oncoimmunology. 2016;5(4): e1122157.
17. Sydney R. Gordon, Roy L. Maute, Ben W. Dulken. PD-1 expression by tumor-associated macrophages inhibits phagocytosis and tumor immunity. Nature. 2017;545(7655):495–499.
18. RoyNoy, Jeffrey W.Pollard. Tumor-associated macrophages: From mechanisms to therapy. Immunity. 2014;41(1): 49–61.
19. Caroline Boudousquie, Giovanna Bossi, Jacob M. Hurst. Polyfunctional response by ImmTAC (IMCgp100) redirected CD8+ and CD4+ T cells. Immunology. 2017;152(3). 425–438.
20. Yao Y，Jeyanathan M，Haddadi S. Induction of autonomous memory alveolar macrophages requires T cell help and is critical to trained immunity. Cell. 2018;175(6):1634-1650.
21. Peter J. Murray, Judith E. Allen, Subhra K. Biswas. Macrophage activation and polarization: nomenclature and experimental guidelines. Immunity. 2014;41(1): 14–20.
22. Gorjana Rackov, Enrique Hernández-Jiménez, Rahman Shokri. p21 mediates macrophage reprogramming through regulation of p50-p50 NF-κB and IFN-β. J Clin Invest.2016;126(8): 3089–3103.
23. Fang J, Li YH, Li XH. Effects of melatonin on expressions of β-amyloid protein and S100β in rats with senile dementia. Eur Rev Med Pharmacol Sci. 2018;22(21):7526-7532.
24. Yao J, Du Z, Li Z. 6-Gingerol as an arginase inhibitor prevents urethane-induced lung carcinogenesis by reprogramming tumor supporting M2 macrophages to M1 phenotype. Food Funct. 2018;9(9):4611-4620.
25. Nefertiti C. DuPont, Kehui Wang. Validation and comparison of luminex multiplex cytokine analysis kits with ELISA: Determinations of a panel of nine cytokines in clinical sample culture supernatants. J Reprod Immunol. 2005;66(2): 175–191.
26. Du G, Liu Y, Li J. Hypothermic microenvironment plays a key role in tumor immune subversion. Int Immunopharmacol.2013;17(2):245-253.
27. Linxin Liu, Hong Li, Zhenzhen Guo. The combination of three natural compounds effectively prevented lung carcinogenesis by optimal wound healing. PLoS ONE. 2015;10(11): e0143438.
28. Du Z, Zhang S, Lin Y. Momordicoside G Regulates Macrophage Phenotypes to Stimulate Efficient Repair of Lung Injury and Prevent Urethane-Induced Lung Carcinoma Lesions. Front Pharmacol.2019;10:321.

29. Sica A, Invernizzi P, Mantovani A. Macrophage plasticity and polarization in liver homeostasis and pathology. Hepatology.2014;59(5):2034-2042.
30. Kataki A, Scheid P, Piet M. Tumor infiltrating lymphocytes and macrophages have a potential dual role in lung cancer by supporting both host-defense and tumor progression. J Lab Clin Med. 2002;140(5):320-328.
31. Neidhart M, Pajak A, Laskari K. Oligomeric S100A4 is associated with monocyte innate immune memory and bypass of tolerance to subsequent stimulation with lipopolysaccharides. Front Immunol.2019;10:791.
32. Li K, Yang F, Zhang G, et al. AIK1, A Mitogen-Activated Protein Kinase, Modulates Abscisic Acid Responses through the MKK5-MPK6 Kinase Cascade. Plant Physiol. 2017;173(2):1391-1408.
33. Li K, Yang F, Miao Y, Song CP. Abscisic acid signaling is involved in regulating the mitogen-activated protein kinase cascade module, AIK1-MKK5-MPK6. Plant Signal Behav. 2017;12(5):e1321188.
34. Pang Y, Li J, Qi B. Aquaporin AtTIP5;1 as an essential target of gibberellins promotes hypocotyl cell elongation in Arabidopsis thaliana under excess boron stress. Funct Plant Biol. 2018;45(3):305-314.
35. Chai LQ, Meng JH, Gao J. Identification of a crustacean β-1,3-glucanase related protein as a pattern recognition protein in antibacterial response. Fish Shellfish Immunol. 2018;80:155-164.
36. Sun Y, Huang T, Hammarström L. The Immunoglobulins: New Insights, Implications, and Applications. Annu Rev Anim Biosci. 2020;8:145-169.
37. Chai H, Guo J, Zhong Y. The plasma-membrane polyamine transporter PUT3 is regulated by the Na+ /H+ antiporter SOS1 and protein kinase SOS2. New Phytol. 2020;226(3):785-797.
38. Yang Y. Cancer immunotherapy: harnessing the immune system to battle cancer. J Clin Invest. 2015;125(9):3335-3337.
39. Joy Hsu, Jonathan J, Hodgins. Contribution of NK cells to immunotherapy mediated by PD-1/PD-L1 blockade. J Clin Invest.2018;128(10): 4654–4668.
40. Burton DGA, Stolzing A. Cellular senescence: Immunosurveillance and future immunotherapy. Ageing Res Rev. 2018;43:17-25.
41. Frank Vari, David Arpon, Colm Keane. Immune evasion via PD-1/PD-L1 on NK cells and monocyte/macrophages is more prominent in Hodgkin lymphoma than DLBCL. Blood. 2018; 131(16): 1809–1819.
42. Alberto Mantovani, Federica Marchesi, Alberto Malesci.Tumor-Associated Macrophages as treatment targets in oncology. Nat Rev Clin Oncol. 2017;14(7): 399–416.
43. Chayanon Ngambenjawong, Heather H. Gustafson, Suzie H. Pun. Progress in tumor-associated macrophage (TAM)-targeted therapeutics. Adv Drug Deliv Rev. 2017;114: 206–221.
44. Boris Novakovic, Ehsan Habibi, Shuang-Yin Wang. β-glucan reverses the epigenetic state of LPS-induced immunological tolerance. Cell.2016;167(5): 1354–1368.
45. Degao Chen, Jing Xie, Roland Fiskesund. Chloroquine modulates antitumor immune response by resetting tumor-associated macrophages toward M1 phenotype. Nat Commun. 2018;9: 873.

46. Felgner S, Kocijancic D, Frahm M. Bacteria in cancer therapy: Renaissance of an old concept. Int J Microbiol. 2016;2016: 8451728.
47. Maryam A. Shetab Boushehri, Mona M. A. Abdel-Mottaleb, Arnaud Béduneau. A nanoparticle-based approach to improve the outcome of cancer active immunotherapy with lipopolysaccharides. Drug Deliv. 2018;25(1): 1414–1425.
48. Lokody. Anticancer therapy: Bacterial treatment for cancer. Nat Rev Drug Discov. 2014;13(10):726.
49. Minghui Yang, Jingli Tao, Hao Wu. Responses of transgenic melatonin-enriched goats on LPS stimulation and the proteogenomic profiles of their PBMCs.Int J Mol Sci.2018;19(8): 2406.
50. B.F. McAdam, I.A. Mardini, A. Habib. Effect of regulated expression of human cyclooxygenase isoforms on eicosanoid and isoeicosanoid production in inflammation. J Clin Invest. 2000;105(10): 1473–1482.
51. West MA, Heagy W. Endotoxin tolerance: A review. Crit Care Med.2002;30(1 Supp):S64-S73.
52. Sanchez-Cantu L, Rode HN, Christou NV. Endotoxin tolerance is associated with reduced secretion of tumor necrosis factor. Arch Surg. 1989;124(12):1432-1435.
53. Karp CL, Wysocka M, Ma X. Potent suppression of IL-12 production from monocytes and dendritic cells during endotoxin tolerance. Eur J Immunol. 1998;28(10):3128-3136.
54. Leon N Schulte, Ana Eulalio, Hans-Joachim Mollenkopf. Analysis of the host microRNA response to Salmonella uncovers the control of major cytokines by the let-7 family. EMBO J. 2011;30(10): 1977–1989.
55. Sifat Maria, Rebekah M. Samsonraj, Fahima Munmun. Biological effects of melatonin on osteoblast/osteoclast cocultures, bone, and quality of life: Implications of a role for MT2 melatonin receptors, MEK1/2, and MEK5 in melatonin-mediated osteoblastogenesis. J Pineal Res.2018;64(3): 10.
56. Biliana Marcheva, Kathryn Moynihan Ramsey, Ethan D. Buhr. Disruption of the clock components CLOCK and BMAL1 leads to hypoinsulinemia and diabetes. Nature. 2010;466(7306): 627–631.
57. Mauricio F. Farez, Ivan D. Mascanfroni, Santiago P. Méndez-Huergo. Melatonin contributes to the seasonality of multiple sclerosis relapses. Cell. 2015;162(6): 1338–1352.
58. Brzezinski A. Melatonin in humans. N Engl J Med.1997;336(3):186-195.
59. V Raghavendra, V Singh, A V Shaji. Melatonin provides signal 3 to unprimed CD4+ T cells but failed to stimulate LPS primed B cells. Clin Exp Immunol. 2001;124(3): 414–422.
60. Carrillo-Vico A, Lardone PJ, Naji L. Beneficial pleiotropic actions of melatonin in an experimental model of septic shock in mice: regulation of pro-/anti-inflammatory cytokine network, protection against oxidative damage and anti-apoptotic effects. J Pineal Res.2005;39(4):400-408.
61. Lijie Zhai, Stefani Spranger, David C. Binder. Molecular pathways: targeting IDO1 and other tryptophan dioxygenases for cancer immunotherapy. Clin Cancer Res. 2015;21(24): 5427–5433.
62. Ana C. R. Moreno, Bruna F. M. M. Porchia, Roberta L. Pagni. The combined use of melatonin and an indoleamine 2,3-Dioxygenase-1 inhibitor enhances vaccine-induced protective cellular immunity to

HPV16-associated tumors. Front Immunol. 2018;9: 1914.

63. Johnathan G Lyon, Nassir Mokarram, Tarun Saxena. Engineering challenges for brain tumor immunotherapy. Adv Drug Deliv Rev. 2017;114: 19–32.
64. Soumaya Ben Khedher, Monica Neri, Florence Guida. Occupational exposure to endotoxins and lung cancer risk: results of the ICARE Study. Occup Environ Med. 2017;74(9): 667–679.
65. Virissa Lenters, Ioannis Basinas, Laura Beane-Freeman. Endotoxin exposure and lung cancer risk: a systematic review and meta-analysis of the published literature on agriculture and cotton textile workers. Cancer Causes Control. 2010;21(4): 523–555.
66. Philipp J. Rauch, Aleksey Chudnovskiy, Clinton S. Robbins. Innate response activator B cells protect against microbial sepsis. Science. 2012;335(6068):597–601.
67. Goto S, Sakai S, Kera J. Intradermal administration of lipopolysaccharide in treatment of human cancer. Cancer Immunol Immunother. 1996;42(4):255-261.
68. Pawelek JM, Low KB, Bermudes D. Bacteria as tumour-targeting vectors. Lancet Oncol.2003;4(9):548-556.
69. Berger M, de Boer JD, Bresser P. Lipopolysaccharide amplifies eosinophilic inflammation after segmental challenge with house dust mite in asthmatics. Allergy. 2015;70(3):257-264.

Figures

Fig.1

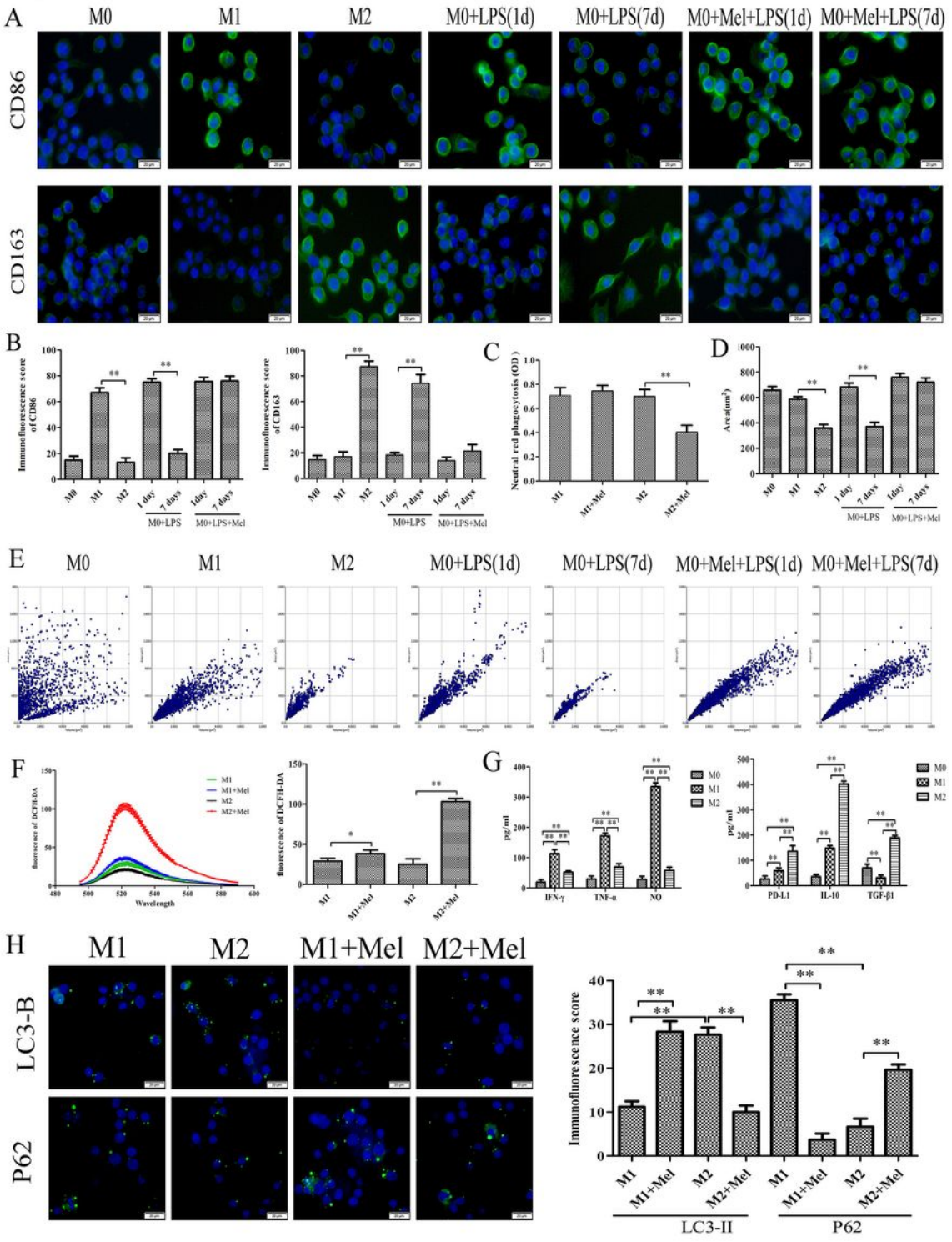

Figure 1

There is a difference between M1-like and M2-like neutrophils. M1-like and M2-like macrophages were induced respectively by LPS and IL-10 from Raw264.7 macrophages. (A) and (B) Macrophages CD86 and CD163 expression was analysed by FITC-conjugated anti-mouse CD86 and CD163 staining (n=5, 40×). (C) Macrophages phagocytosis detected by neutral red (n=5, 40×). (D) and (E) Macrophages morphological changes analysed by laser holographic cell imaging and analysis system (n=5, 20×).(F)

ROS detected by DCFH-DA (n=5). (G) Supernatant cytokine levels in cell culture (n=5). (H) Cell autophagy as indicated by LC3-B and P62 staining (n=5, 40×). The data present Mean ± SD, the experiments were repeated 3 times, and statistical significance was determined by a t-test. *P < 0.05, **P < 0.01 . Mel:Melatonin.

Fig.2

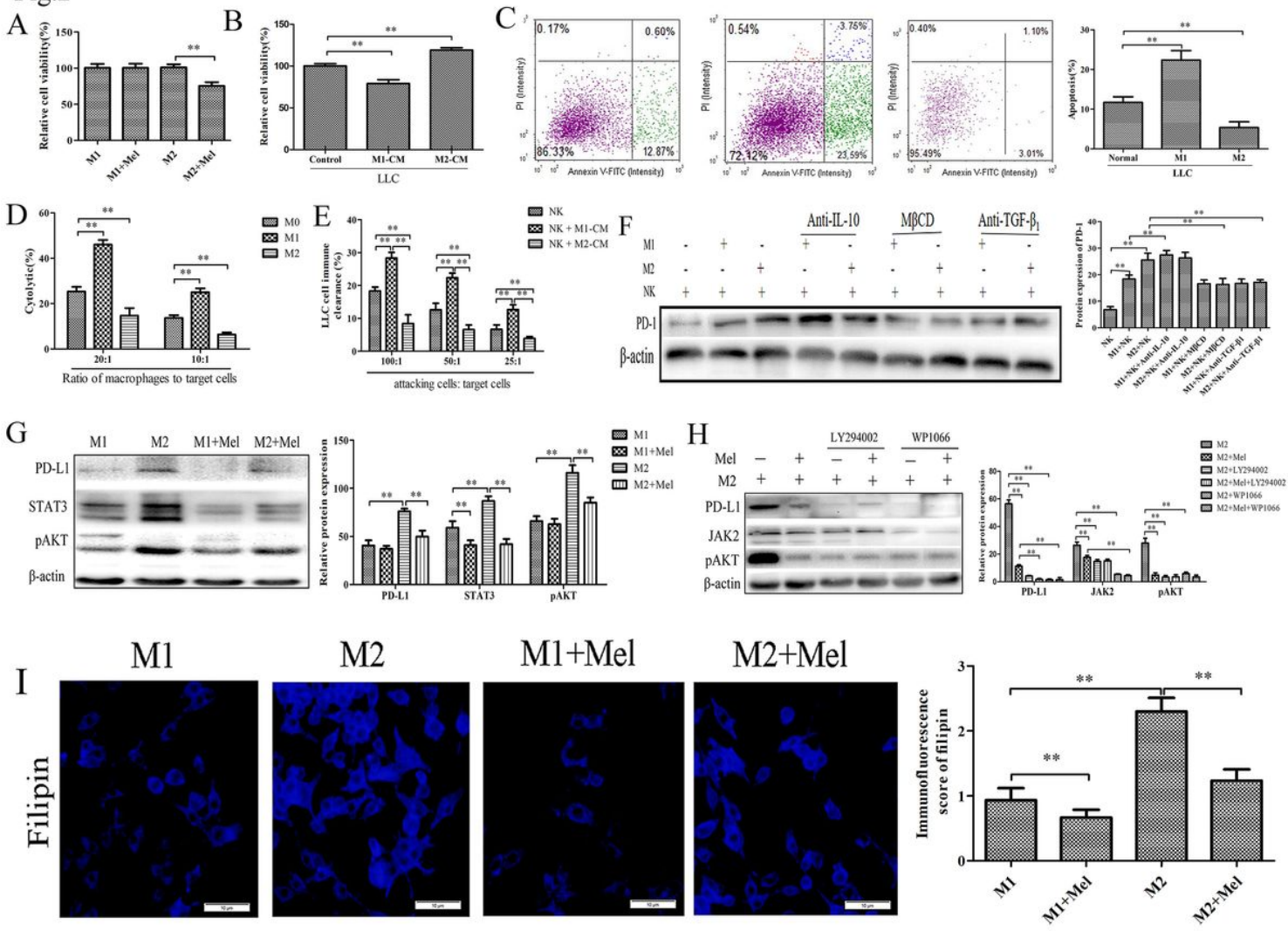

Figure 2

M1-like and M2-like macrophages had different effects on LLC cells and NK cells. (A) Macrophages cell viability detected by MTT assay (n=5). (B) LLC cell viability detected by MTT assay (n=5). (C) Cell apoptosis detected by the Annexin V-FITC apoptosis kit (n=5). (D) Cytolytic activity (n=5). (F), (G)and(H) Protein expression levels of PD-1, STAT3 and pAKT examined by Western blotting (n=5). (I) Lipid raft examined by filipin (n=5). (F) PD-1 production in NK cell supernatant(n=5). (E) NK cell immune clearance. The data present Mean ± SD, the experiments were repeated 3 times, and statistical significance was determined by a t-test. *P < 0.05, **P < 0.01 . Mel:Melatonin.

Fig.3

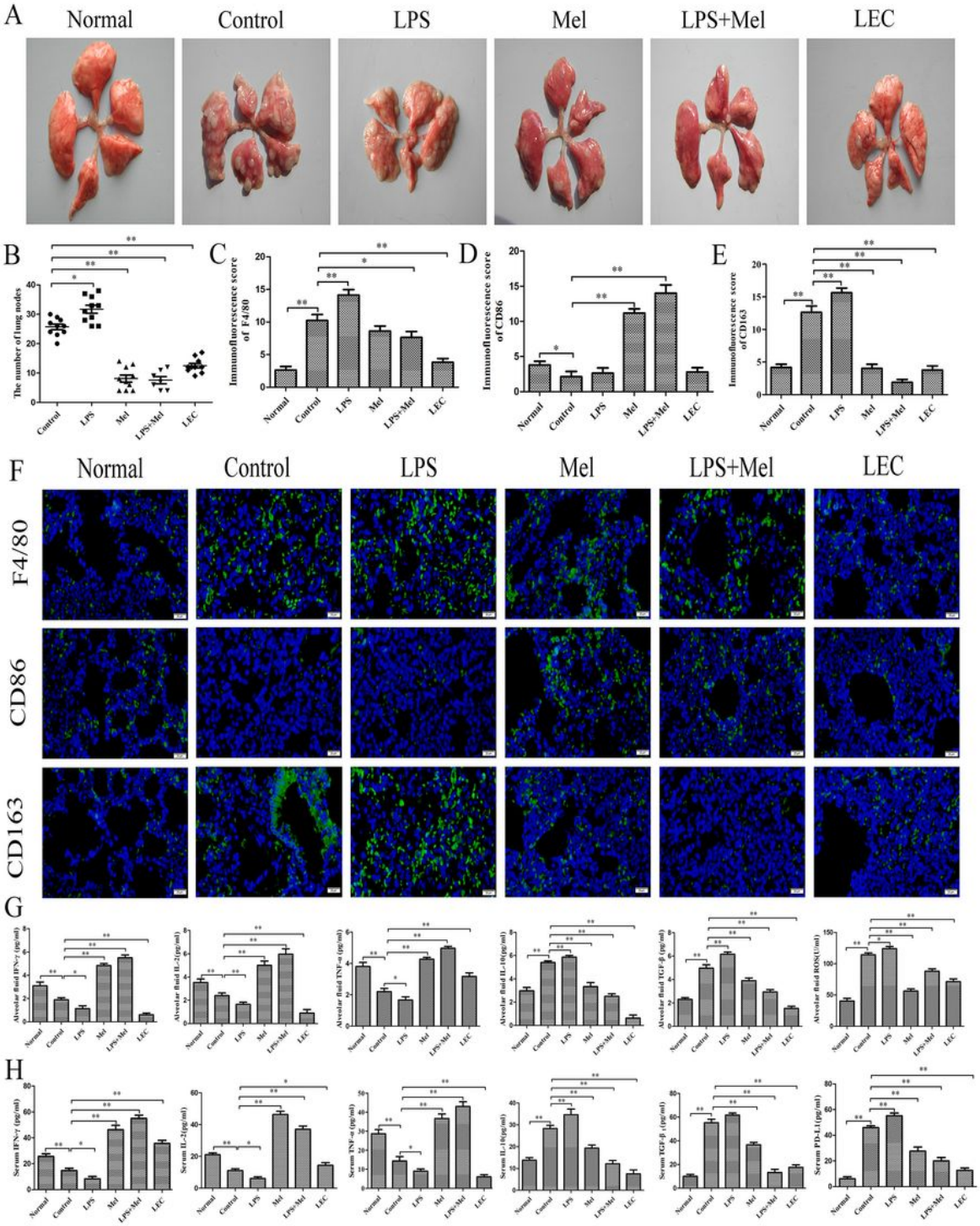

Figure 3

Macrophages affect urethane-induced lung carcinogenesis. (A) The whole lung (n=10). (B) The number of lung nodes (n=10). (C),(D),(E) and (F) Alveolar macrophages indicated by immunofluorescence (n=5, 40×). (G) and (H) Serum and alveolar cytokine levels in urethane-induced lung cancer mice (n=5). The data present Mean ± SD, the experiments were repeated 3 times, and statistical significance was determined by a t-test. *P < 0.05, **P < 0.01 .Mel:Melatonin.

Fig.4

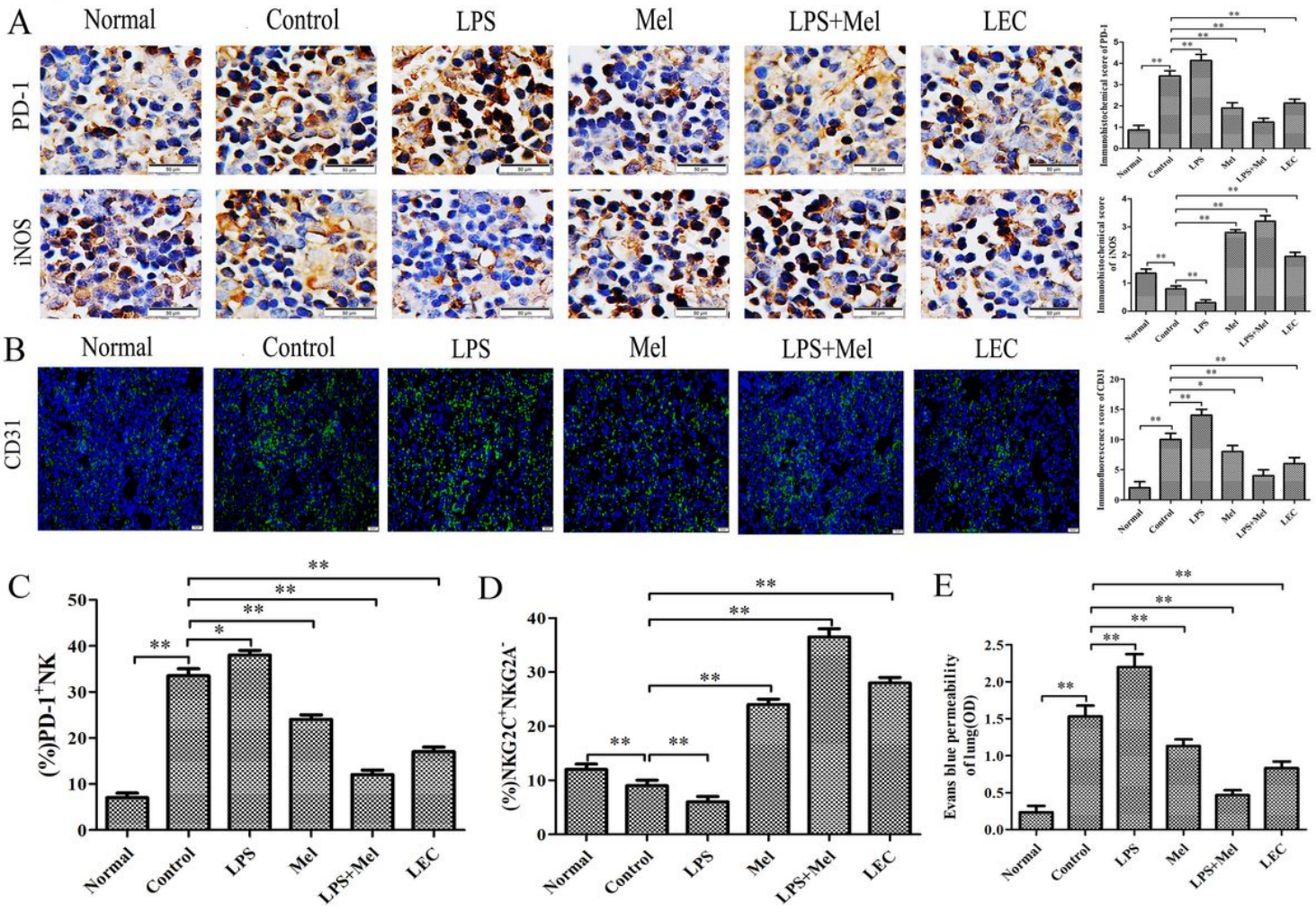

Figure 4

Melatonin maintains macrophage immune function in urethane-induced lung carcinogenesis. . (A) PD-1 and iNOS expression in lung tissues examined by immunohistochemistry (n=5, 40×). (B) Lung tissue CD31 expression indicated by immunofluorescence (n=5, 40×). (C) Spleen NK cell rate (n=6). (D) Spleen memory NK cell rate (n=5). (E) Lung tissue permeability to Evans blue (n=5). The data present Mean ± SD, the experiments were repeated 3 times, and statistical significance was determined by a t-test. (a) *P < 0.05, **P < 0.01. Mel:Melatonin.

Fig.5

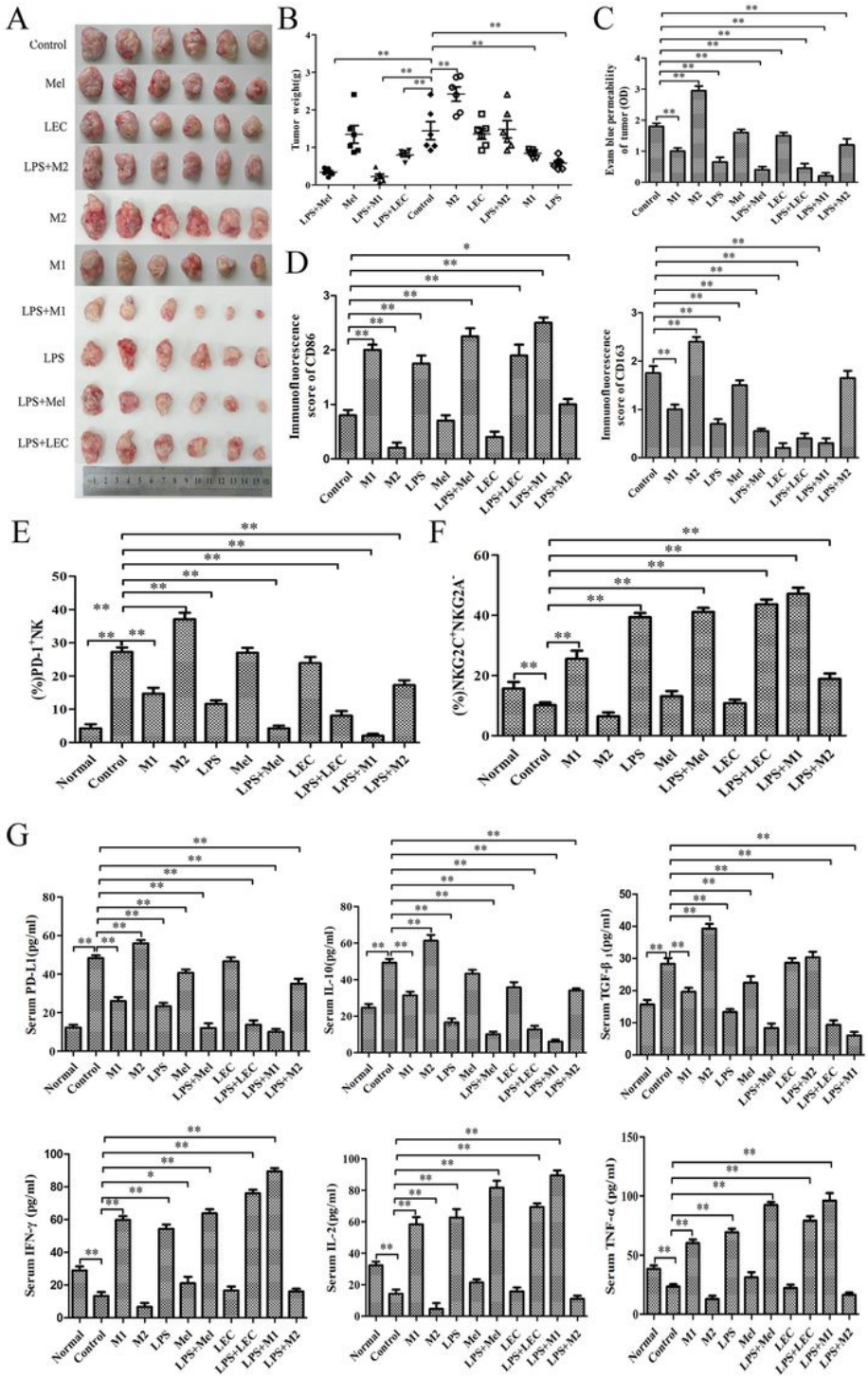

Figure 5

Melatonin maintains macrophage M1 phenotype to keep tumour secondary immunity. (A) and (B) Tumour and tumor growth curve in a H22 tumour allotransplantation model (n=6). (C) Tumour tissue permeability to Evans blue (n=6). (D) Peritoneal macrophage immunophenotypes indicated by immunofluorescence (n=6). (E) Spleen NK cell PD-1+ rate (n=6). (F) Spleen memory NK cell rate (n=6). (G)

Serum cytokine levels (n=6). The data present Mean ± SD, the experiments were repeated 3 times, and statistical significance was determined by a t-test. *P < 0.05, **P < 0.01 Mel:Melatonin.

Fig.6

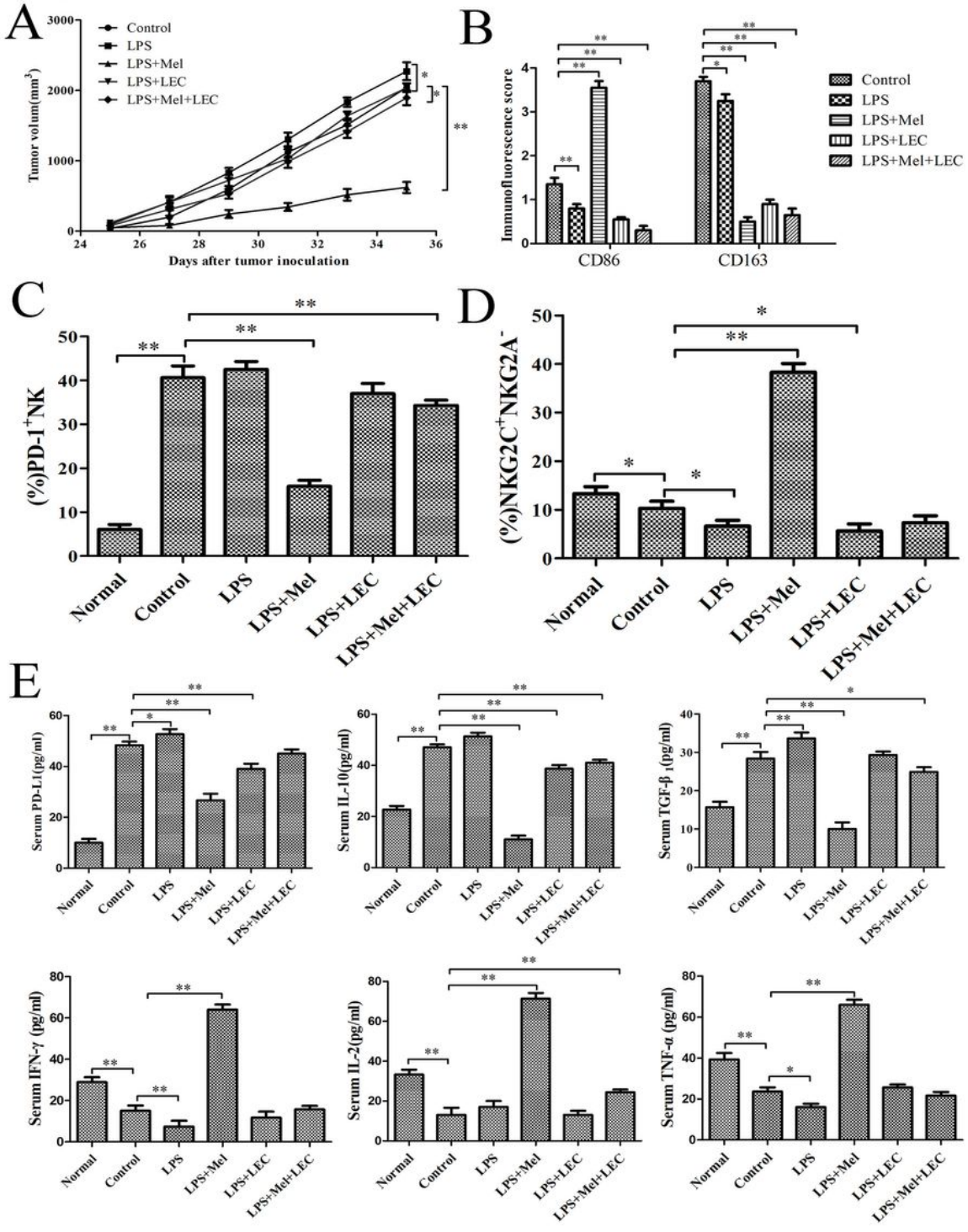

Figure 6

Melatonin maintains macrophage M1 phenotype to keep tumour immune memory. (A) Tumour growth curve in a H22 tumour rechallenge immune study. (n=6). (B) Peritoneal macrophage immunophenotypes indicated by immunofluorescence (n=6, 40×). (C) Spleen NK cell PD-1+ rate (n=6). (D) Spleen memory NK

cell rate (n=6). (E) Serum cytokine levels (n=6). The data present Mean ± SD, the experiments were repeated 3 times, and statistical significance was determined by a t-test. *P < 0.05, **P < 0.01.Mel:Melatonin.

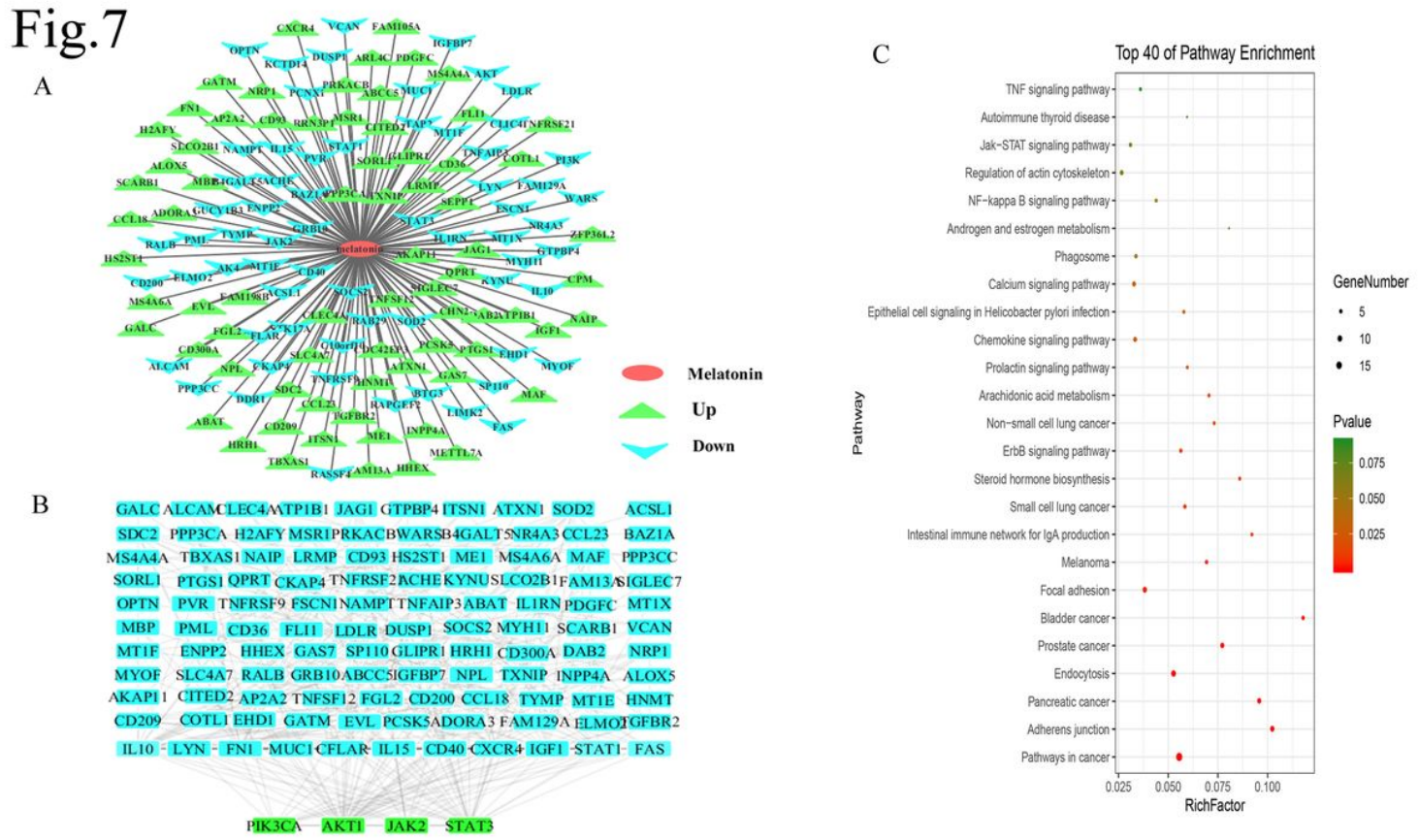

Figure 7

The potential targets of melatonin in regulating macrophages analysed by network pharmacology and a predictive role of NLR in chemotherapy sensitivity of cancer patients. (A) and (B) The potential targets of melatonin in regulating macrophages and the PPI network. (C) KEGG enrichment analysis performed by DAVID and visualized by ehbio.

Fig.8

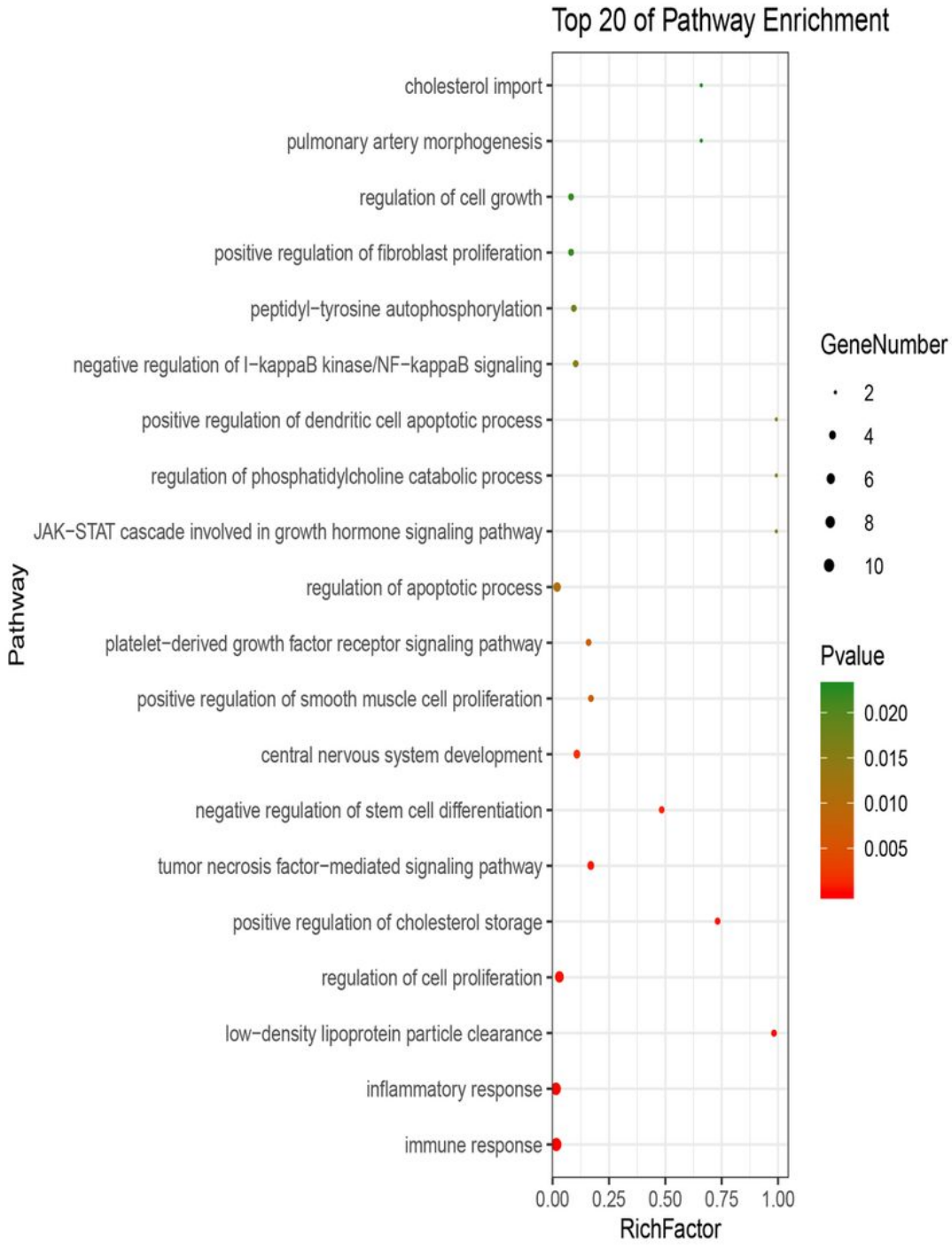

Figure 8

GO enrichment analysis performed by DAVID and visualized by ehbio .

Fig 9

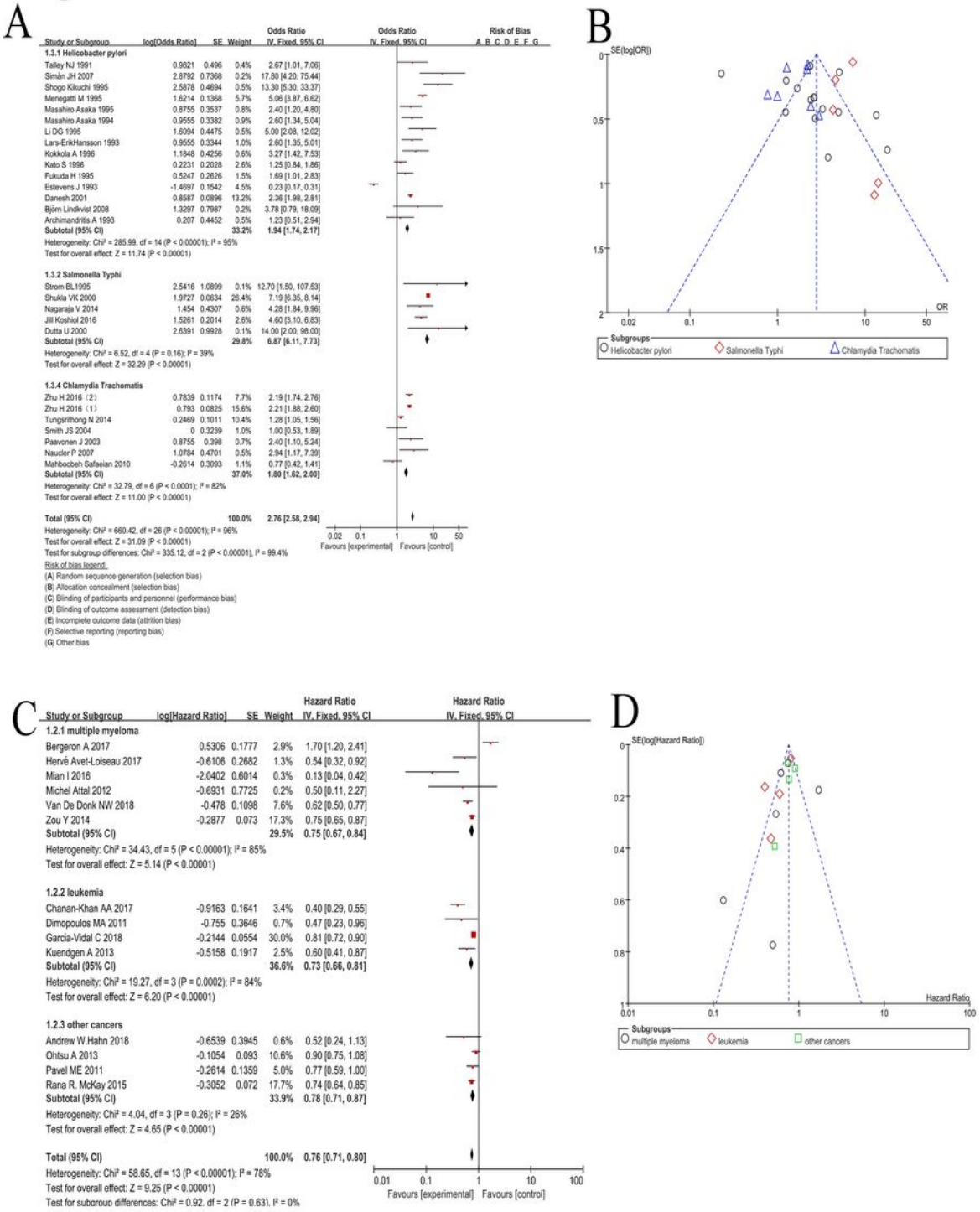

Figure 9

A predictive role of bacterial infection in risk of carcinogenesis and cancer survival. (A) (B) Effect of bacterial infection on carcinogenesis in the meta-analysis shown as the forest map and the funnel diagram. (C) (D) Effect of bacterial infection on cancer survival in the meta-analysis shown as the forest map and the funnel diagram.